

Total System Error (TSE) Analysis of Helicopter Procedure in an Alpine Environment Flying Advanced RNP Procedures

Heinz Wipf, *AIRNAV CONSULTING Zurich, Switzerland*

Biography (IES)

Heinz Wipf received his engineering diploma in communication and computer science from the Technikum Winterthur Switzerland. He holds three degrees in post-graduate studies from the Swiss Institute of Technology Zurich ETHZ and Lausanne EPFL in electromagnetic compatibility, applied statistics and a master in management, technology and economics respectively. His working experience includes 35 years with the Swiss Air Navigation Services Ltd. in fields of radio navigation, business development, statistics and operational - technical program management. Before he has been with Siemens in research and development working on advanced private branch exchanges. While active as an assistant professor and lecturer for more than 20 years in electrical communication systems at the College of Engineering Zurich and for navigation systems at the Zurich University of Applied Science in Winterthur, he also taught a variety of short courses.

Elected founding president of the Swiss Air Traffic Technical Association, he currently also serves as a board member of the Swiss Association of Aeronautical Sciences and the Institute of Navigation. As a longstanding and senior member of the Institute of Electrical and Electronics Engineers he founded and chairs the Swiss-Chapter on Aerospace Electronic Systems. His numerous other memberships in professional organizations include the AOC, AIAA and aerosuisse. In his capacity as a subject matter expert he has participated in a number of international working groups within ICAO and Eurocontrol. He holds several patents and is an expert witness on oath in Austria. He currently runs his own company AIRNAV CONSULTING in Zurich as managing director and senior ANS-expert.

Abstract

This paper shows data analytical results gathered in flight trials in the course of introducing PBN. Switzerland has extensively researched and probed into IFR helicopter operations under varying conditions and thereby reached beyond the envelope of OEM-certified limits for the aircraft. Light helicopters in use for disaster relief, SAR and emergency medical services operated by private or state authorities show limited capability to carry extensive avionics due to the weight of other mission critical on-board equipment. With the necessity of an ever-widening operational scenario, all-weather capability becomes a key element in specific helicopter operations, whereas high maneuverability allows reduced track distances in time critical operations.

Flight trials using HeliFIS¹ in the Swiss Alps at 1800m AMSL and above had, among other objectives the gathering of empirical lateral (cross track) Navigation System Error (NSE) and Total System Error (TSE) of an auto-piloted light helicopter with only a GNSS NAV sensor.

All flights were based on GNSS/SBAS operated in VMC in airspaces with no ground based navigation means. Other trial objectives were the helicopter's FMS/AP capability to fly RNP0.1 AR APCH, RF intermediate segments and LPV - PinS APCH and DEP. The helicopter AW109SP is certified for LPV, LNAV/VNAV, LNAV and RNP0.3/all phases-of-flight was demonstrated and is currently under review by the OEM.

Introduction

When introducing PBN in Switzerland a considerable portion of the program was directed towards IFR helicopter operations. Light helicopters in use for disaster relief, SAR and emergency medical services operated by private or state authorities show limited capability to carry extensive avionics due to the weight of other mission critical on-board equipment. With the

¹ Helicopter Flight Inspection System

necessity of an ever-widening operational scenario, all-weather capability becomes a key element in specific helicopter operations. The use of GNSS as a primary navigation source is therefor obvious.

When starting to fly advanced IFR procedures in demanding mountainous terrain SBAS quickly became the GPS augmentation of choice. As a consequence the total system error (TSE) was reduced significantly.

At the same time ICAO's IFPP² started to look closer into IFR helicopter procedures and the lateral buffer values stemming from the design of fixed wing aircraft procedures [2]. These to be applied buffer values are of course related to the probability density functions of the helicopter TSE. Apparently these empirical data sets are globally in short supply. Getting notice from the IFPP, we set out to collect this data as part of PBN helicopter flight trials in the Swiss Alps. Apart from data collecting we also undertook the necessary steps in data analysis. Thereby outliers in the statistical data sets were discovered. These outliers have for many years spurred discussions about the tails of probability density functions and their parameters. Given the data sets acquired during the helicopter flight trials, hypothesis and possible explanations for the outliers are discussed.

Situation

Procedure design uses lateral buffers consuming airspace that either is not in existence³ or is to be used for other air traffic.⁴ These buffers are based on fairly old empirical data.⁵

Any flight path s can be described as a mass point's trajectory in three dimensions x, y, z , that is $\in \mathbb{R}^3$. The mass point is typically located at the aircraft's center of gravity.

$$x = f\langle t \rangle, y = f\langle t \rangle, z = f\langle t \rangle$$

where

$$ds\langle t \rangle = \left(dx\langle t \rangle^2 + dy\langle t \rangle^2 + dz\langle t \rangle^2 \right)^{\frac{1}{2}} \quad \text{and} \quad s\langle t \rangle = \int \left(dx\langle t \rangle^2 + dy\langle t \rangle^2 + dz\langle t \rangle^2 \right)^{\frac{1}{2}} dt$$

The physical laws governing such a trajectory have been described by Newton in the 17th, namely his second law of motion.

$$\vec{F} = m \cdot \vec{a}\langle t \rangle = m \cdot \frac{d}{dt} \vec{v}\langle t \rangle = m \cdot \frac{d^2}{dt^2} \vec{s}\langle t \rangle$$

where F is the force exercised on the airframe, m is the mass of the aircraft and a is the acceleration, v the speed and s the trajectory of the aircraft. For the sake of simplicity let \mathbb{R}^3 be reduced to \mathbb{R}^2 and $s\langle t \rangle$ split up in its orthogonal components $x\langle t \rangle$ and $y\langle t \rangle$.⁶ The problem to solve thus is to find a class of trajectories or 3d curves for which the curvature is a polynomial function of the length $s\langle t \rangle$. A cost function for optimization in discussion for helicopter operation is the altitude, which of course is governed by the minimum height above terrain.

PROBLEM STATEMENT - ANALYTICAL CONSIDERATIONS

While civil engineering in railroad (late 19th century) and later in highway construction (middle of 20th century) has applied physical curves for quite some time [8], aviation has obviously not felt the necessity to do so. The fact is that a straight segment interfacing a circle segment in a tangent fashion has no second derivative of $s\langle t \rangle$.⁷ In consequence to Newton's 2nd law the accelerations would be undefined.

The author discovered this shortcoming in instrument procedure design at a PBN workshop back in 2009⁸ for the first time, while other authors [7 p 3] addressed it already in 2006.

² Instrument Flight Procedure Panel

³ E.g. terrain

⁴ Military

⁵ Collision Risk Modeling (CRM) - ICAO Doc 9274-AN/904 1st Edition 1980

⁶ The problem space remains in \mathbb{R}^3 as can be seen from the mathematical notation, as t is a parameter and not an additional dimension.

⁷ "Der Übergang von einer Geraden in einen Kreisbogen ist immer sprunghaft, wenn dies auch bei sehr großen Radien oder geringen Fahrgeschwindigkeiten nicht ohne weiteres spürbar ist. Die Eisenbahnen, welche gegen Ende des letzten Jahrhunderts große Fahrgeschwindigkeiten erreichten, begannen schon damals ihre Kurven zu überhöhen und zwischen Gerade und Kreft eine Übergangskurve einzuschalten." from [8 p 1] for the a copy of the original see annex.

⁸ PBN Summit in Seattle

Helicopters [9 p 162, 177] and modern jet fighters are inherently partly unstable - a feature which typically supports the aircraft's agility in flight. Higher maneuverability allows reduced track distances, which is an advantage in time critical operations. Low pass filtering for damping would therefore impair the responsiveness of the auto-piloted aircraft and is therefore no viable option. This static instability makes those aircraft the platform of choice to study the response due to sudden abrupt autopilot commands.

The abrupt reaction of a helicopter in flight is clearly discernible, if passing a fix, which joins a straight leg with a circular turn. Albeit the difference in flight dynamics, a statically stable fixed wing aircraft will eventually perform a smoother flight. The resulting error in the flight path will be locally of a lesser magnitude and will persist for a longer interval before and after the fix.

Today's flight procedure design suggests curved flight trajectories especially for advanced approach and departure. The standardized design is called Radius-to-Fix, whereas a straight-line segment is connected to another segment being part of a circle circumference defined by its radius and the coordinates of the start and end waypoint or fix. The coding of the flight management system (FMS) is done in a likewise fashion.

Analyzing the situation, calculus is of no help⁹, because an analytical solution is not possible (for the mathematical proof see the annex). Yet it is possible to apply a trick⁹ to approximate the effect such a transition has on the acceleration of a mass point. The trajectories can be discretized in time. Hence double differences of $s(t)$ can be applied. This results in an approximation of the acceleration (right graphics) to which the mass point is subjected while trying to follow one of the typical trajectories (left graphics) below.

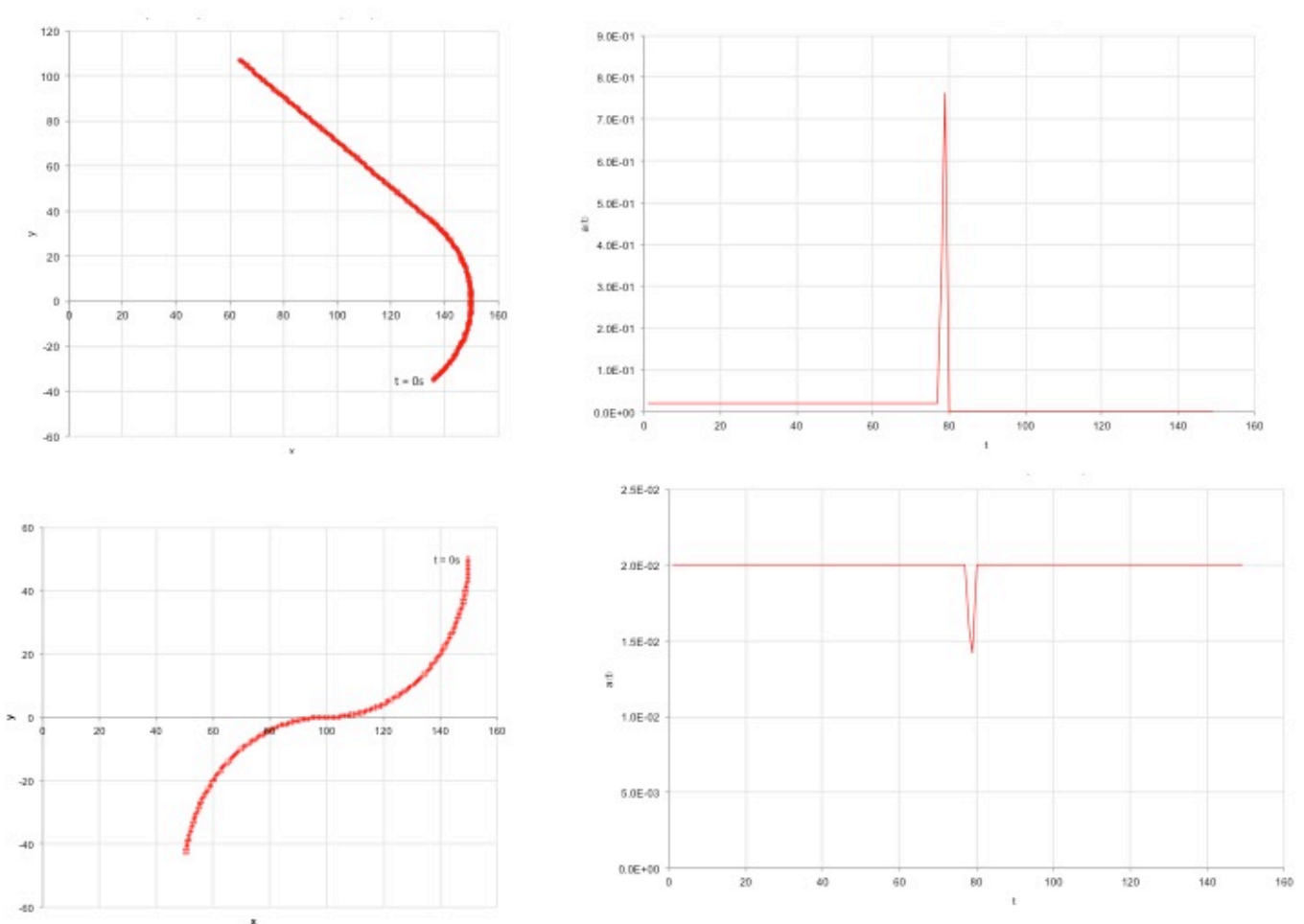


Figure 1 – Discrete double differencing of a radius-to-fix and a radius-to-radius transition.

Different combinations are obviously irrelevant, for the detrimental effects of undefined accelerations are retained.

⁹ Finding the derivative of a function by numerical methods is resorted to when the methods of differential calculus are inapplicable.

INSTRUMENT FLIGHT PROCEDURES

The flight trials in the Swiss Alps at 1800m AMSL and above had, among other objectives the gathering of empirical lateral (cross track) Navigation System Error (NSE) and Total System Error (TSE) of an auto-piloted light helicopter with only one kind of NAV sensor. The chart in Fig. 2 covers an exemplary part of the trajectories flown during those trials. The procedure for RWY 21 is not shown in Fig. 1 to avoid clutter, but is referenced under [5].

The flight guidance was based on GNSS/SBAS. All flights were operated in VMC under IFR and in airspaces with no ground based navigation means.

A detail of importance for the sequel is that the trajectory flown consisted of Radius-to-fix and straight legs. A detailed account of possible transitions is found below..

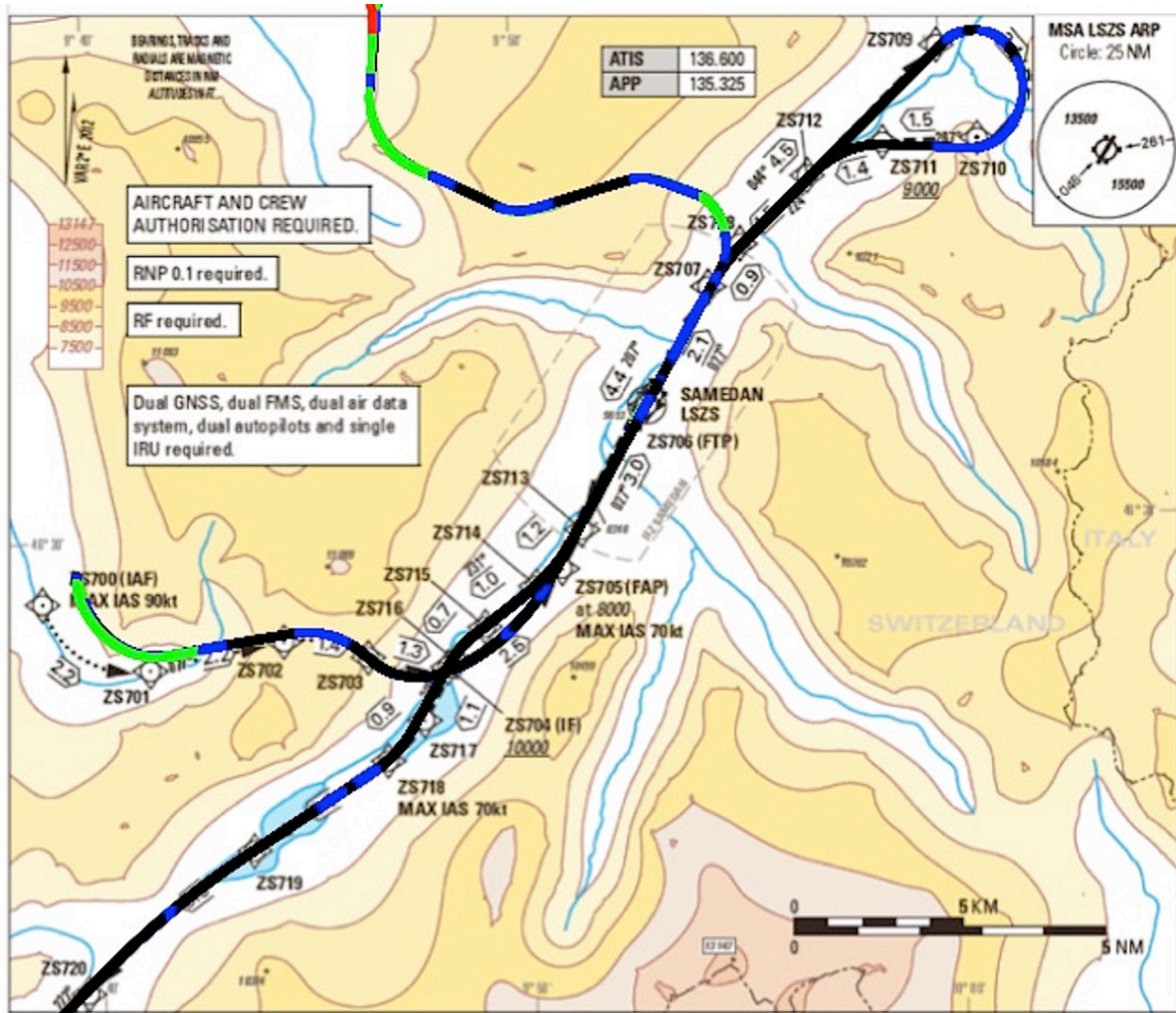


Figure 2 - Procedure chart SAMEDAN LSZS RWY03 [4] and all runs (nr2...nr9) superposed as overlay with their lateral TSE color-coded. $|\text{rnavCrossTSE}| > 100\text{m}$, $> 30\text{m}$, $> 10\text{m}$, $< 10\text{m}$.

It is noticeable for 95% of all $|\text{rnavCrossTSE}|$ values were $< 36.37\text{m}$ or $< 0.0196\text{nm}$, which would suffice for RNP0.02 at least empirically.

FLIGHT TRIALS

The flight trial program for the implementation of the helicopter procedure SAMEDAN LSZS RNAV (RNP) RWY 03/21 HELICOPTER CAT H in 21.04.2016 also comprised a helicopter flight inspection and validation. Other trial objectives were the helicopter's FMS/AP capability to fly RNP0.1 AR APCH, RF intermediate segments and LPV - PinS APCH and DEP.

The flight trials themselves were part of the European PBN Rotorcraft Operations under Demonstration project (PROuD).¹⁰ The aircraft to carry out the flight inspection was a Rega helicopter AW109SP. Rega /Swiss Air Ambulance as the main emergency medical service (EMS) provider in Switzerland and firmly engaged in promoting and applying advanced IFR helicopter is operating this aircraft. The organization operates a fleet of some 20 aircraft for EMS in Switzerland. The helicopter is IFR certified. The helicopter's avionic suite features two primary GNSS receivers and is certified for LPV, LNAV/VNAV and LNAV. RNP0.3/all-phases-of-flight was demonstrated and currently is under review by the OEM. The flight characteristics state a minimum speed of 55kt if flown under autopilot and IFR, while under LPV one is allowed to reduce to 45kt with steepest LNAV/VNAV and LPV glide path angle of 9 degrees. With the autopilot engaged the rule of thumb indicates a maximum bank angle of $v/10 + 7 v$ in kt. This results in 120kt: 19°, 90kt: 16°, 70kt: 14° (see also Fig. 9). The minimum turn radius is 800 ft and 360° in 2 min which equals 3°s^{-1} .

Flight Check Instrumentation

The flight check used the specifically developed inspection system HeliFIS by Aerodata. The system recorded among other data all relevant parameters of the GNSS/SBAS¹¹ signals. The recordings permitted a post flight ASCII data extraction which is due to the availability of corresponding laboratory equipment at Flight Calibration Services GmbH (FCS). Flight data from primary GPS and FMS were recorded on board the aircraft with help of fixed installed quick access recorder¹² and are also available for data analysis. For a complete list of processed variables see the annex. A detailed review on the equipment and its aircraft integration is found in [3].

Meteorological conditions

The meteorological condition has relevance to the trials in as far as the flights had to be conducted under VMC. Additionally adverse wind conditions especially gusty cross winds could have had an uncontrolled impact on the navigation performance of the helicopter. However the flight meteorological data¹³ for the day shows no noteworthy circumstances. Wind speeds in the valley were between 0 and 14kt and between 160° to 220°.

DATA ANALYSIS

One general issue in test planning is the different aspect in lateral error assessment. It seems unclear whether the TSE induced buffers have to protect a single flight or all flights passing a certain critical or governing obstacle. The interest of a pilot obviously touches the first one. The interest of an airport or an air navigation service provider may be the latter.

A single realization asks for a longitudinal study. The service aspect at defined points in space however needs a cross sectional approach. The longitudinal error-probability-density-distribution of course vary from a cross sectional one. While for the first case the lateral errors of a realization¹⁴ are not be iid¹⁵, it may well be the case for the second one¹⁶.

Pooling the data of longitudinal realizations may be a way out of this dilemma by making use of the central limit theorem in statistics. This would then also give support to the tradition in aviation of assuming a normal distribution of navigational errors.

Flight Trial Results

All runs were flown by the 4-axis autopilot of the AW109SP. However not all runs from 1...9 were taken into account. Run nr1 had to be abolished due to pilot intervention and runs nr8 and nr9 were outside of the test scope. Nevertheless they are incorporated for completeness in some of the figures below. All runs 2...7 with their varying length are shown in the annex. The data sets comprise 90020 positions sampled as time series along the trajectories of uneven lengths. The basic information on the data sets is summarized in Tab. 1.

¹⁰ See the yet unpublished EU-report for further details. Refer to the PROuD SESAR Joint Undertaking. Demonstration Report (B1) 2016 LSD.02.09

¹¹ GPS and EGNOS

¹² Avionics miniQAR MKIII

¹³ METAR courtesy of Meteo Suisse

¹⁴ Approach or departure

¹⁵ Independent and identically distributed

¹⁶ Central limit theorem in statistics

Run		nr2	nr3	nr4	nr5	nr6	nr7	nr8	nr9	total
TSE	Samples	4090	19917	5154	12821	11758	5400	7618	23262	90020
	Proportion	5%	22%	6%	14%	13%	6%	8%	26%	100%
NSE	Samples	496	2063	600	1363	1257	621	843	2407	9650
	Proportion	5%	21%	6%	14%	13%	6%	9%	25%	100%

Table 1 – Sample sizes and proportion of the different runs

In respect to the data analysis runs nr8 and nr9 as indicated above have been removed from the data set. The detailed evaluation below therefore includes only the runs in Tab. 2.

Run		nr2	nr3	nr4	nr5	nr6	nr7	nr8	nr9	total
TSE	Samples	4090	19917	5154	12821	11758	5400			59140
	Proportion	7%	34%	9%	22%	20%	9%			100%
NSE	Samples	496	2063	600	1363	1257	621			6400
	Proportion	8%	32%	9%	21%	20%	10%			100%

Table 2 Reduced Data set used for the detailed analysis

The TSO GPS receiver providing data for evaluating the NSE has a $1s^{-1}$ sampling rate while the HeliFIS calculates the position at $10s^{-1}$ for the TSE. This fact leads to NA's¹⁷ in the NSE data entry and explains the differences in sample size in the tables above.

Fig. 3 below presents the individual lateral TSE results for runs 2 through 9 as time series. The horizontal axis units are tenths of a second; the vertical axis units are meters of lateral TSE.

¹⁷ NA for Not Available

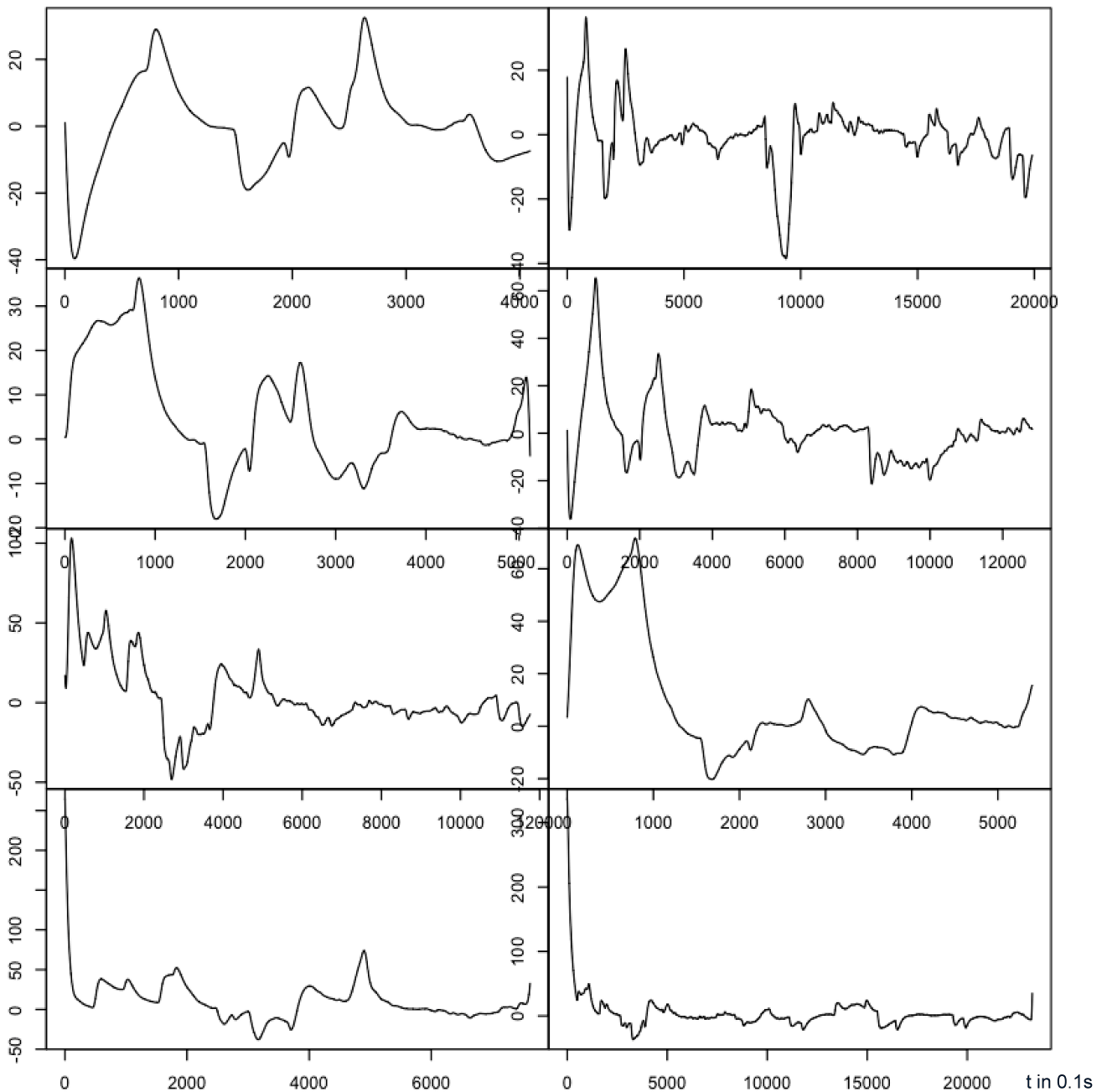


Figure 3 – Overview of the TSE on all runs (nr2 - nr9) on record from top left to right as time series. The sampling interval is 0.1s.

The time series exhibit a tendency of a progressive reduction of the lateral TSE as a function of time or along the trajectory. This effect has been brought to the attention of the OEM. An explanation has not yet been forthcoming. In general, one notices a more important TSE in the initial phase of the runs especially nr4 – nr9. This behavior was already visible in the first series of flight trials of 20th – 22th July in 2015. The corresponding recordings for run nr8 and nr9 have a problem just right at the start, which renders the statistical analysis difficult. They are part of a different set and do not belong to this series of flight trials.^{18 19} As a consequence of the comments in the footnotes, runs nr8 and nr9 have been removed in the sequel of this paper.

¹⁸ Ref email 30.05.2016 pilot T. Gnägi/Rega - The flight technical view confirms that the deviation at waypoint ZS780 may have an explanation in the short intercept in combination with its fly-by coding. Moreover the leg before ZS780 has not been defined yet. It is therefore not clear under which angle one should approach the waypoint.

Fig. 4 displays the empirical probability densities of the lateral TSE for each of the individual relevant runs shown in Fig. 3a and some empirical distributions compare favorably with the theoretical graphs shown in Fig. 3b

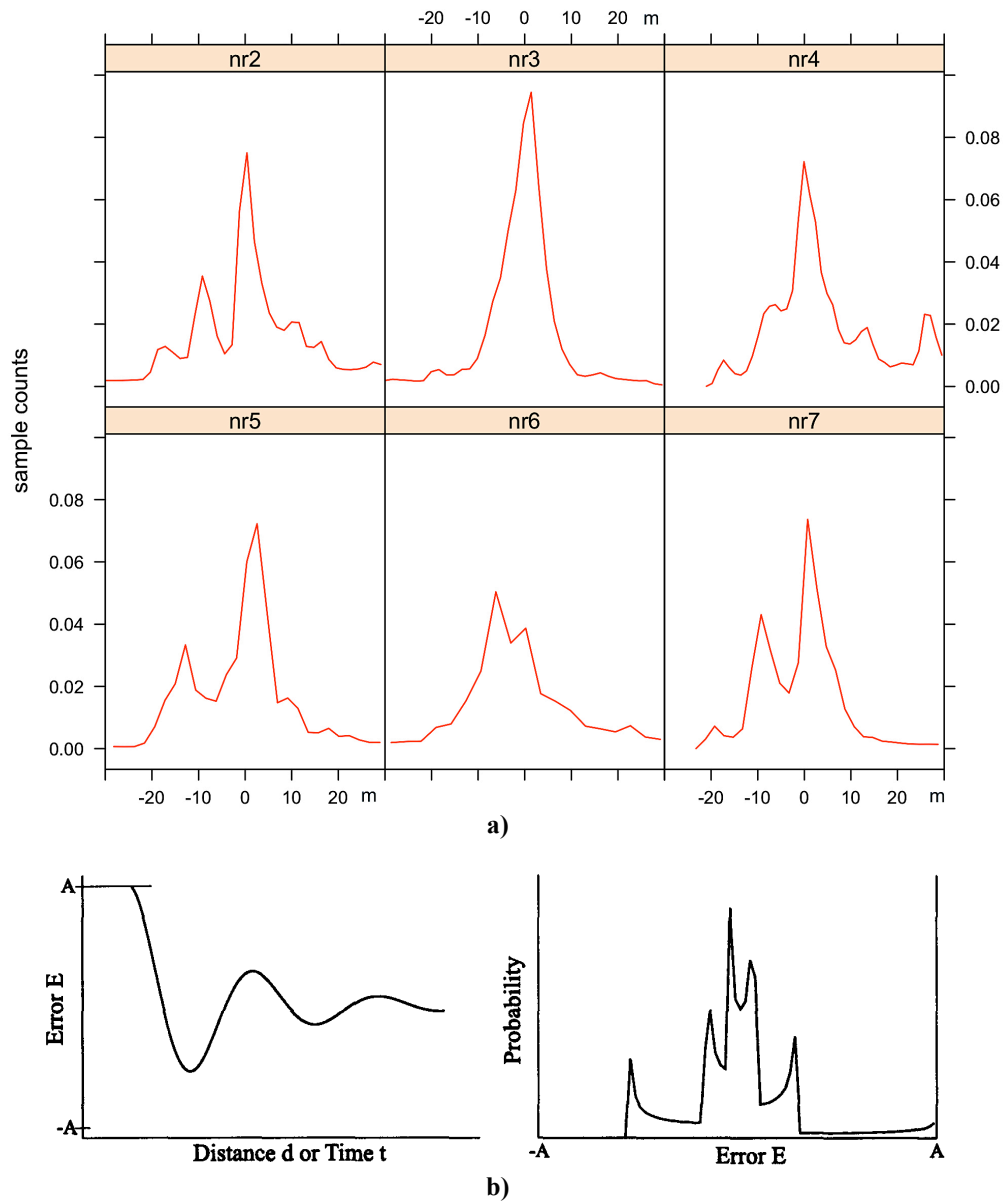


Figure 4 – Empirical densities in m^{-1} (y- axis) of the lateral TSE in m (x- axis) (a) and theoretical error distributions (b) resulting from the interaction of a control loop typically employed in an autopilot. Courtesy M. Scaramuzza²⁰

Due to the second order control loops²¹ generally employed in autopilot applications, it must be underlined that an individual flight trajectory has the tendency to exhibit a bi-modal U-shaped PDF representing lateral errors along the flight trajectory. This effect is visible in Fig. 3 nr2, 4, 5, 7 and to a lesser degree in nr6. The densities resemble the ones derived in [6 p 28 et seq.].²² For a more indebt view Stengel in [10 p 436, 442] provides an overview and mathematical treatise of general flight control systems.

¹⁹ Ref email 24.05.2016 FCS flight inspector M. Schwendener -- The first waypoints BIVIO and ZS780 are coded as fly-by. Depending when the FMS is armed, different fly by distances will result. At BIVIO the intercepts are in line with the first legs. At ZS780 the intercept angles are $>30^\circ$. In my opinion the FMS reacted normally. It is questionable whether it should be used for data analysis.

²⁰ From [6 p 30 Fig. 3.10]

²¹ Private communication, Dr. A. Smerlas Certification Directorate - EASA

²² Fig. 3.8, 3.9 and 3.10

Fig. 5 shows boxplots for all 8 runs (nr2 - nr 9). In (a) with outliers and (b) with the outliers removed. Outliers are marked with small circles above and below the whiskers. The vertical axis is the rnavCrossTSE in m. Box sizes are in proportion to the square root of the sample size for the respective run and comprise 50% of all data. The horizontal bar in the box marks the median value of the sample set. The whiskers above and below the box extend to the extremes.

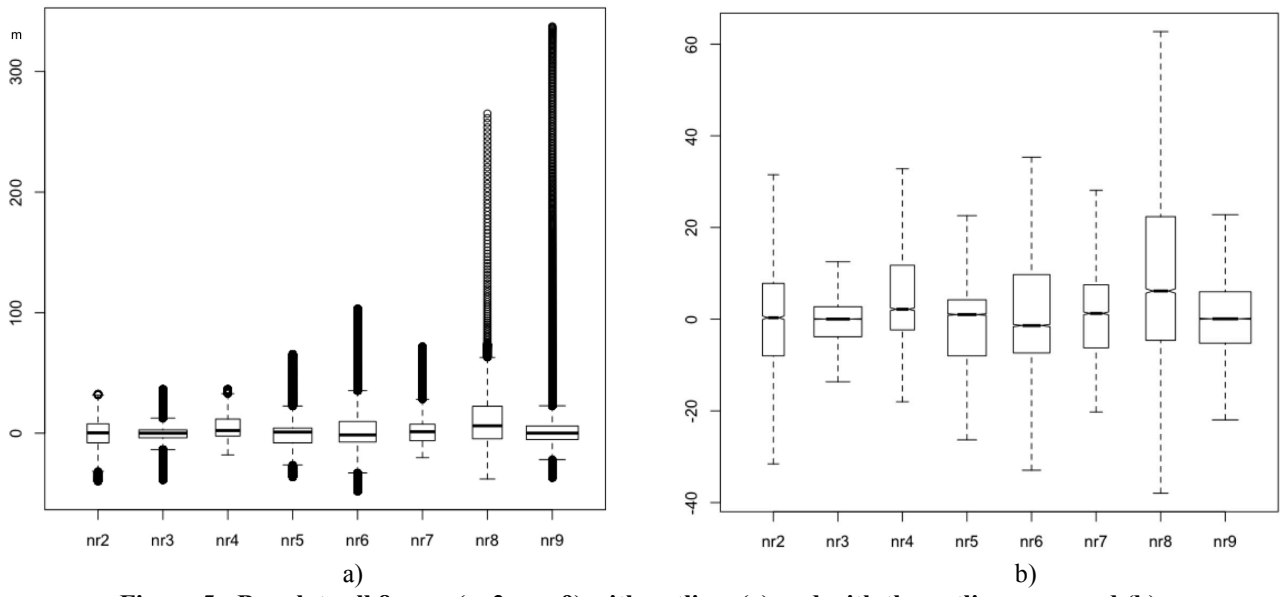


Figure 5 - Boxplots all 8 runs (nr2 - nr 9) with outliers (a) and with the outliers removed (b).

All runs display outliers. With the exception of run nr3 the outliers were found to be asymmetrically distributed, which is also reflected in the skewed distribution in Fig. 4. Again runs nr8 and nr9 display the largest outliers, which is due to the initial excursions shown in Fig. 3. The boxplots one would expect to see from typical errors should rather look like Fig 4 b), where the same data like in a) is displayed, but the outliers are suppressed.

Pooling longitudinal data

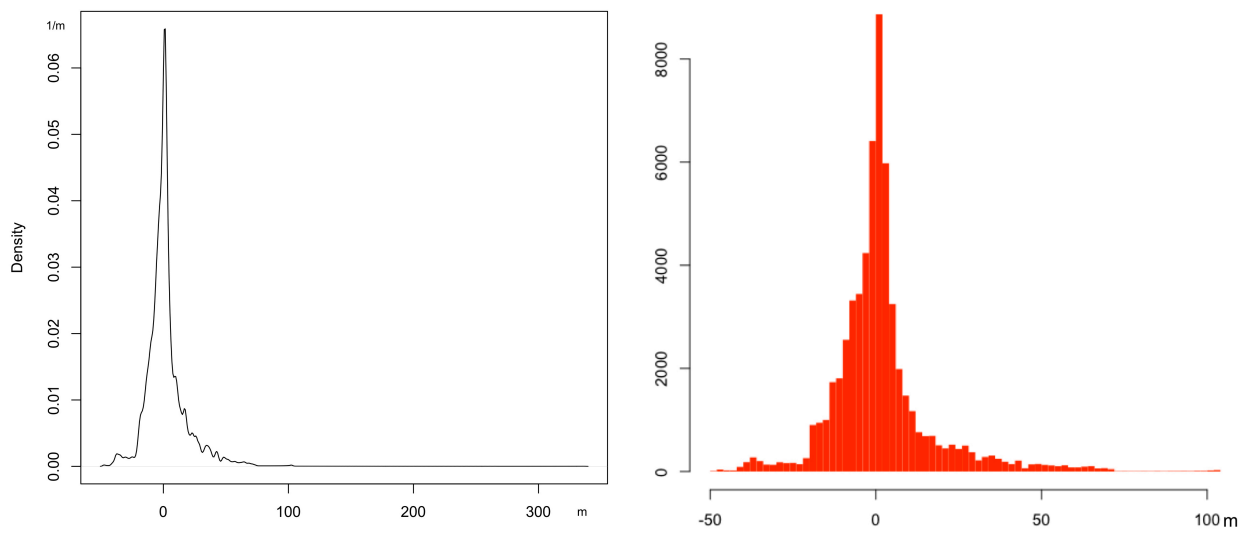


Figure 6 - Probability density of runs nr2 ... nr7 showing the rnavCrossTSE in m. The bandwidth is 0.7763 with a Gaussian kernel and the corresponding histogram comprising 59140 observations.

As can be seen in Fig 4 and 5 most densities are asymmetric. Eventually this fact is also reflected in the pooled data. The TSE distribution is also skewed and does not resemble a normal distribution. The histogram displays the often-cited fat tails not being in accordance with normality nor other parametric distributions.

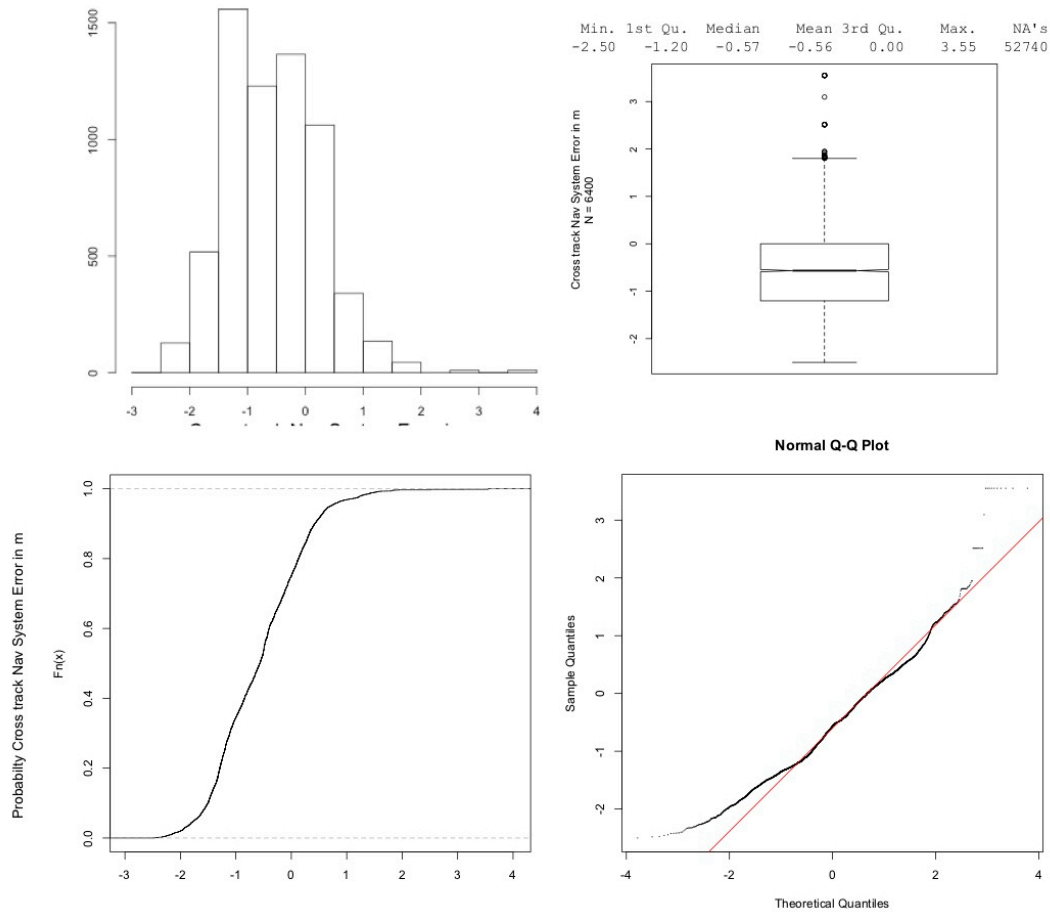


Figure 7 – NSE summary graphs and values of the runs nr2 – nr7

The NSE shows a slight bias in the histogram. The sensor performance under SBAS when flying approach procedures in an alpine valley is rather remarkable²³. Remember the helicopter is certified only to RNP1. Just a few outliers in the boxplot are observed and also visible in the normal Q-Q plot.²⁴ Appreciating the red line in the plot as the theoretical normal quantiles distribution allows for assuming a normal distribution of the navigation errors. This is in accordance with the theory. Despite the fact that the data set failed a formal statistical test²⁵ for normality, and for the sake of the argument, let the empirical cumulating distribution function to the lower left be replaced with the analytical one based on the normal distribution. so to allow the probability estimation of the sensor errors.²⁶ The parameters are easily estimated from the NSE data set.

$$\text{mean}(\text{rnnavCrossNSE}) = -0.564\text{m} \quad \text{and} \quad \text{std} = 0.805\text{m}$$

$$p = \int_{s_{cross}}^{\infty} \frac{1}{\sqrt{2\pi} \cdot \sigma} \cdot e^{-\left(\frac{s_{cross}-\mu}{\sigma}\right)^2} d s_{cross}$$

Then the probability in having a navigation sensor offset laterally of $> 5\text{m}$ would be $p = 2.4\text{E-}12$.

Quite a different situation compared to the NSE is found in Fig. 8 with the TSE. Although the helicopter reaches 31m for 95% of the time the distributions do not render to the assumption of normality. This is clearly visible in the Q-Q plot to the lower right.

²³ $8 < \text{nr of tracked SV's} < 13$ - the count includes 2 SV's EGNOS

²⁴ Quartile-Quartile plot

²⁵ Shapiro-Wilk test of normality

²⁶ Error function erf

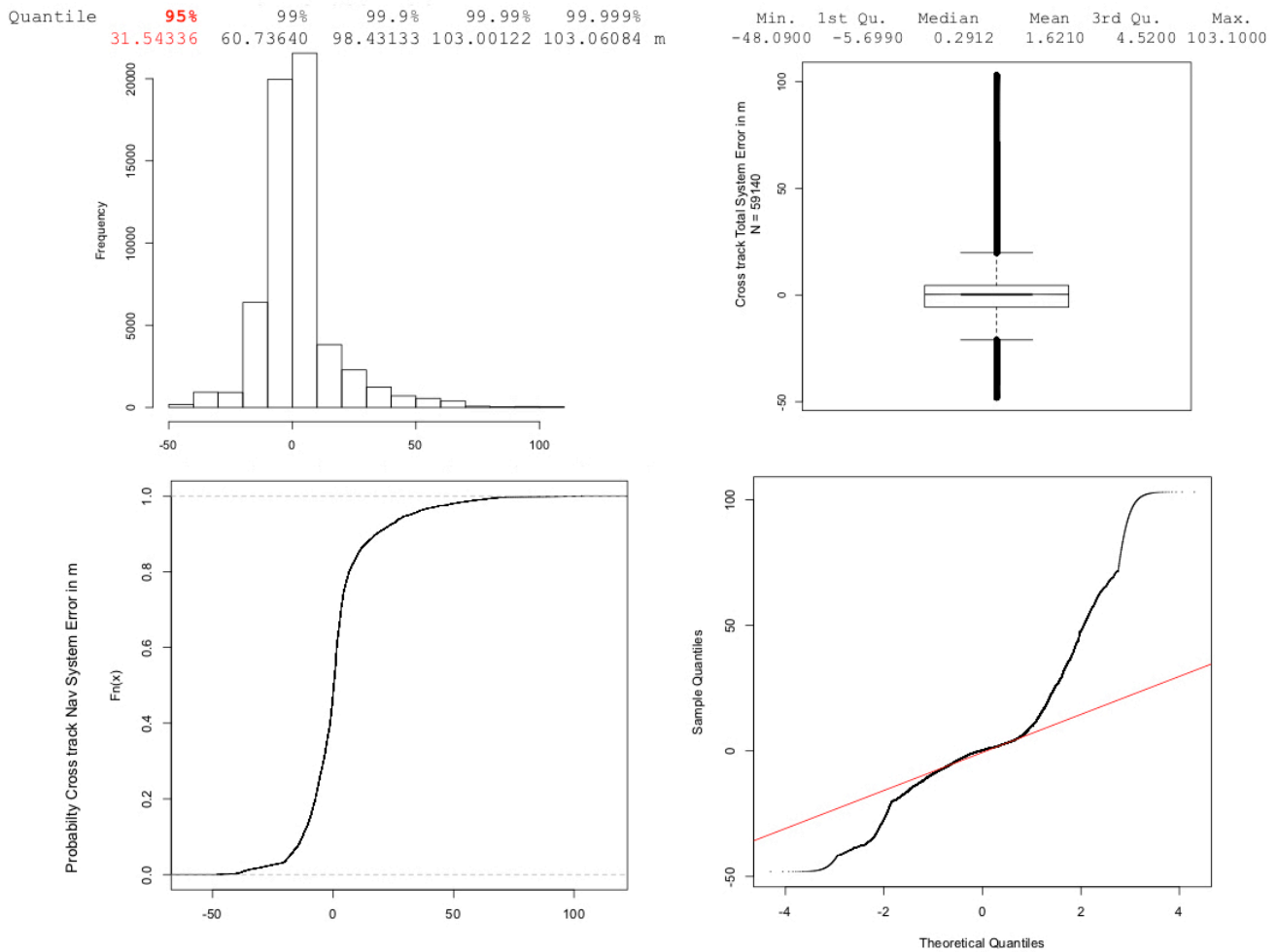


Figure 8 - TSE summary graphs and values of the runs nr2 – nr7

Discussion

So what then are the causes of the skewed empirical probability densities and the countless outliers in the TSE data, although the navigation sensor knows the position of the aircraft fairly accurately? The first point may be attributed to the non-existence of a balanced test plan, resulting in a non-equal distribution of the different transition combination.

Apch'g \	Straight Seg	RF left	RF right
Straight Seg		11	16
RF left	22	6	0
RF right	11	5	0

Table 3 – Sum of transitions combination of flight segments from runs nr2 – nr7 derived from heading information.

Apch'g \	Straight Seg	RF left	RF right
Straight Seg	NA	$j_{1,2}$	$j_{1,3}$
RF left	$j_{2,1}$	$j_{2,2}$	$j_{2,3}$
RF right	$j_{3,1}$	$j_{3,2}$	$j_{3,3}$

Table 4 Test plan for transitions of flight segments.

In order to get rid of a systematic cause for skewed distribution the test plan would have to be a balanced design. This would imply to have trial runs where $j_{m,n}$ are about equal.

A second consideration is contained in the table below. It is exhibiting pairwise scatter plots, the Spearman correlation coefficient including p-values for a statistical test of the correlation between different relevant variables for runs nr2 – nr7 together with the univariate histograms. Units on vertical and horizontal axis are in m with the exception of the pitch/bank angles, which are in degrees. The green line on the scatter plots is the result of a local polynomial regression fitting (Loess).

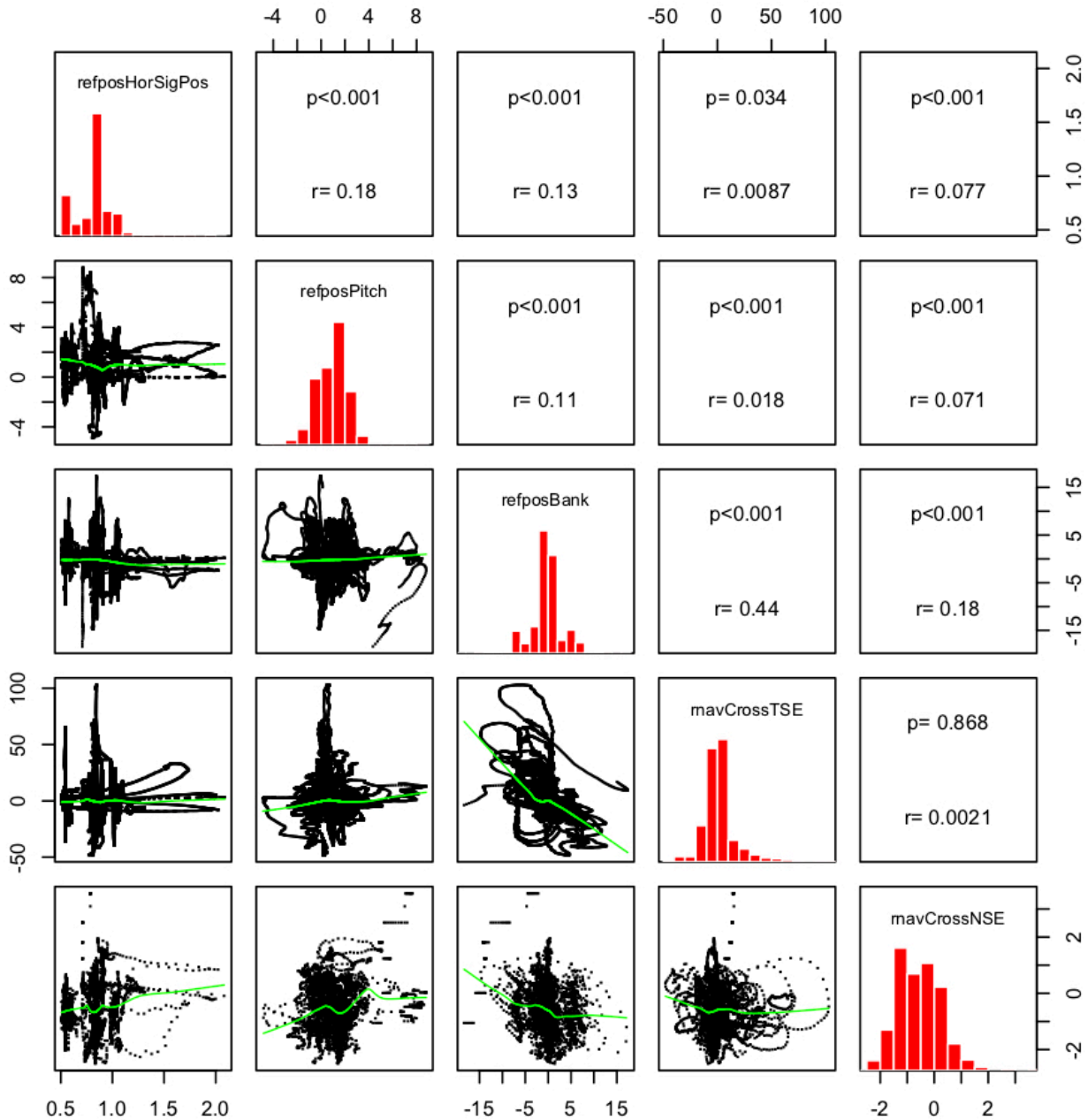


Figure 9 - Pairwise scatter plots with the correlation coefficient between the different variables and the univariate histograms.

One may observe the correlation coefficient of $r = 0.44$ between bank angle and TSE, which gives rise to the hypothesis that the TSE may be related to curves. The navigation system error stays unaffected and correlates neither with the bank angle nor with the TSE, which negates the possibility that masking of space vehicles (SV's) in the mountain valley would be the cause of the TSE²⁷. This hypothesis is further supported by the fact of a missing correlation between the pitch and the NSE. In addition the pitch also seems to have no impact on the TSE only the bank angle does. It should be noted that most p-values show low values, so that H_0 can be rejected and H_A ²⁸ holds on a 0.05 basis with the only exception in the case of TSE and NSE. The slopes of the regression lines reflect the correlations as well. This also means that a correlation between navCrossNSE and rnavCrossTSE cannot be confirmed. Since the TSE is a result of the NSE and the FTE it is remarkable that the FTE seems to be independent from NSE and predominantly determines the TSE. Given the agility of the aircraft and a proper design of the control loops one would expect the FTE to be on the same magnitude or even smaller than the NSE.

²⁷ $8 < \text{nr of tracked SV's} < 13$ - the count includes 2 SV's EGNOS

²⁸ H_A : The true r is not equal to 0 - two-sided test

The Spearman correlation coefficient has been chosen for its robustness towards outliers as encountered in the data sets at hand and because the data must not necessarily come from bivariate normal distribution.

Thirdly observing the time series of the TSE in Fig. 3 and comparing them to the transitions of different procedure elements along the runs, any correlation is not that evident. Thus the time series were transformed in showing the distance on the x-axis and the 1st differences of the TSE on the y-axis. Furthermore the distance from fix to fix were extracted from the procedure charts.

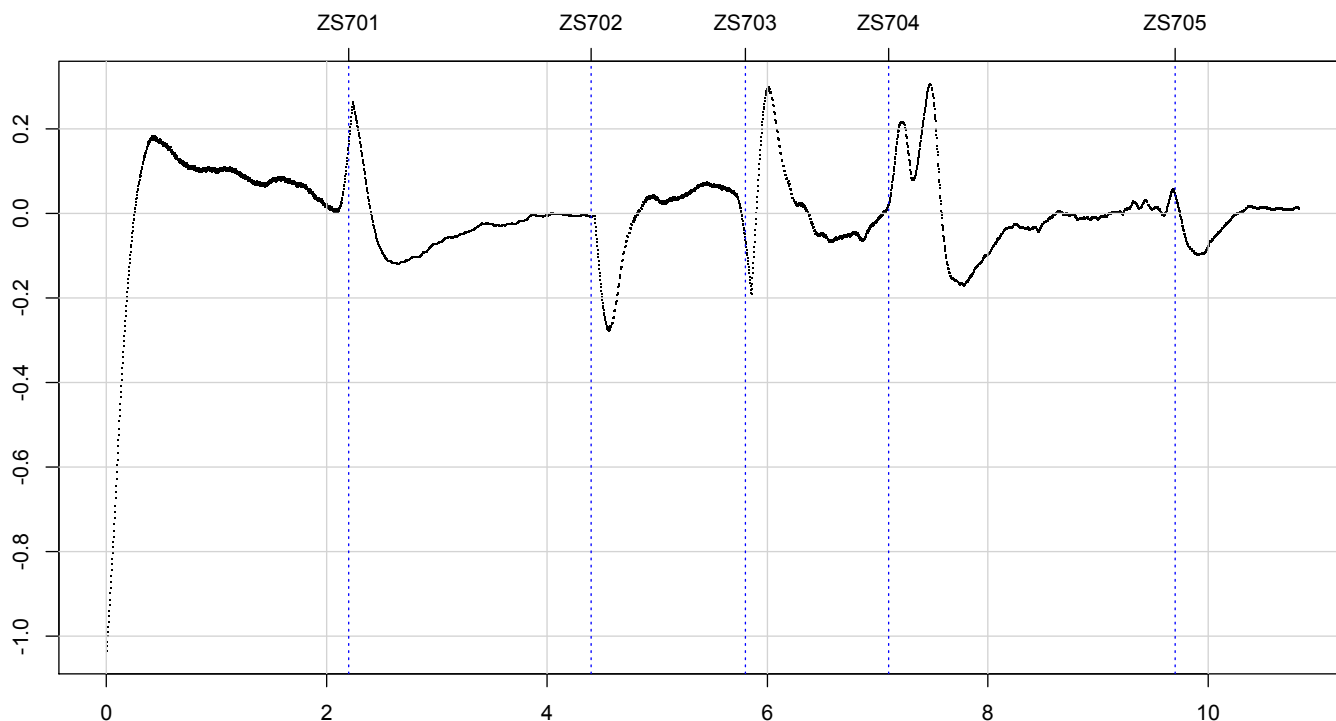


Figure 10 – Run nr2 as an example the y-axis has units m/100ms and the x-axis is in NM.

Since Fig. 10 is exemplary for all runs it clearly shows the systematic impact the various transitions have on the TSE. Naturally if operators fly in an RNAV5 environment these effects will hardly be discernible. In EMS, SAR or other logistic helicopter IFR operations in obstacle rich environments or in demanding terrain, precision flying down to RNP0.3/0.1 is going to be a necessity. The author is of the opinion that properly equipped light helicopters are capable of a much more exigent navigation performance under IFR than that for which they are certified today. This assumes that the trajectories of the procedures are devised in accordance with the laws of physics.

CONCLUSIONS

The lateral GNSS based navigation system error of aircraft over the years is decreasing and with it the TSE. This fact is useful for the design of advanced IFR flight procedures. However whether a flight track is devised as a polygon from fix to fix or a more sophisticated radius-to-fix, such trajectories are considered non-physical. For 1st and 2nd time derivative must exist for a point mass to follow it in theory. A fact, consider Newton’s 2nd law obviously not fulfilled under today’s instrument flight procedure design rules. Literature shows there are neither highways nor high-speed railroad tracks today having such a non-physical layout.

The ICAO IFPP strives to rationalize that the lateral buffers for advanced RNP-procedures must be supported with empirical data in much the same way the CRM²⁹ has been in the past. The point in question is a parametric probability density function that went through a statistical test. Enough data to form empirical density functions would also do, but to get hold of the

²⁹ Manual on the Use of the Collision Risk Model for ILS Operations DOC9274-AN/904 1980

distribution tails the volume of data is considerable, and given the observed enthusiasm demonstrated up until today in providing this empirical data, this endeavor seem to be elusive.

Whether resampling techniques such as the bootstrap and jackknife provide a way out of having insufficient empirical data remains to be analyzed. Newer empirical data must undergo a comprehensive analysis, in order to test statistical hypothesis of given probability-density-functions and thus allow appropriate procedure design. Having analyzed the lateral errors in the horizontal plane, the same considerations would apply of course to the vertical ones.

FUTURE STEPS

In supporting the notion to devise and calculate optimally protected instrument flight procedures, it is of essence to know what kind of a parameterized probability density functions to fit. This results in the availability of an analytical expression for the tails of the distribution. These are difficult to acquire with empirically data, because the costs in resulting flight trials would be excessive. Moreover after data gathering for the CRM in the '80 no further published and accessible global data gathering campaign is known to the author.

To derive parametric densities the empirical data sets have to be free of systematic errors like the ones stemming from a non-physical trajectory design as shown in this paper. A possible way forward is to devise trajectories based on curves having a 1st and 2nd derivative in time of $s(t)$. Those curves are in existence and have been used in other engineering fields [8] for quite some time.

There are a number of candidate functions like simple polynomials, clothoids [8], Bezier curves³⁰ or different splines³¹ to approximate a flight trajectory, while at the same instant posses a 1st and 2nd derivative. Moreover these curves are a part of the tools available in most CAD programs used today by IFP-designers. The IFP designer's product would consequently emerge as an analytical formula representing the flight trajectory in R^3 . The problem for coder and packers of the procedures would then be, how to discretize the analytical function received so to set the sample points correctly and so to allow the programming of the FMS. An example of a trajectory generation process is to be found in [7 p 4].

ACKNOWLEDGMENTS

M. Schwendener FCS provided all the data sets.³² Rega sponsored all helicopter flights. All statistical evaluations were done with R. Data analysis is a courtesy of AIRNAV Consulting Zurich Switzerland. Especially helpful were A. Gruica for the mathematical proof and other colleagues for their comments and suggestions.

REFERENCES

- [1] Newton I. "Philosophiæ Naturalis Principia Mathematica" 1687
- [2] WP 1c-001 First presented: 14-1 Instrument Flight Procedure Panel Working Group Meeting 14-1 WG 2 – Helicopters, Fukuoka, Japan March, 2017
- [3] Schwendener et al "Flight Inspection of Helicopter Procedures in a Challenging Topographic Environment" IFIS 2014
- [4] SAMEDAN LSZS RNAV (RNP) RWY 03 HELICOPTER CAT H 17.02.2017
- [5] SAMEDAN LSZS RNAV (RNP) RWY 21 HELICOPTER CAT H 02.03.2017
- [6] Scaramuzza M. "Systematic Investigations of Error- and System-Modelling of Satellite Based Flight Approaches and Landings in Switzerland" Diss. ETH No. 12892 Zurich 1998
- [7] Smerlas A.J. et al "On the Development of a four-axis AFCS for the Pilot Assistance Experimental System" 2006 dspace-erf.nlr.nl
- [8] Bachmann E. "Die Klothoide als Übergangskurve im Straßenbau" Schweizerische Zeitschrift für Vermessung, Kulturtechnik und Photogrammetrie 1951 Band 49 Heft 6
- [9] Saunders G. H. "Dynamics of Helicopter Flight Hardcover" NY 1975
- [10] Stengel R. "Flight Dynamics" Princeton 20

³⁰ After P. Bézier, at Renault in early 1960 and in a similarly but unpublished work by P. de Casteljaou at Citroen late 1950s and early 1960.

³¹ I.J. Schoenberg in 1946

³² PROuD_Rega_2016_04_21_#2.csv to #9.csv

ANNEX

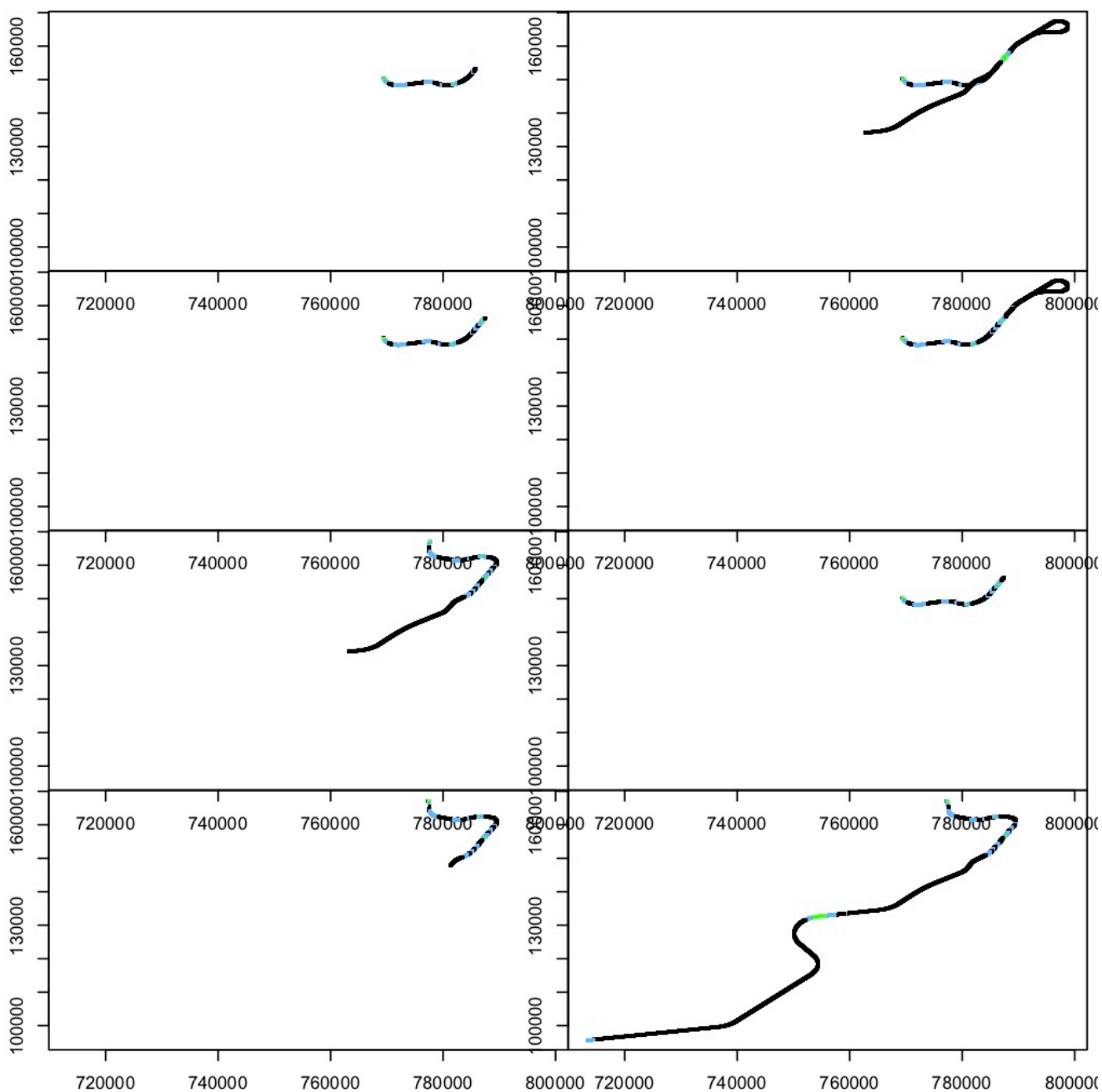


Figure 11 - Overview of all runs (nr2 - nr7) on record from top left to right $|\text{rnavCrossTSE}| = > 100\text{m}, > 30\text{m}, > 10\text{m}, < 10\text{m}$. The Y and X axis are in m reflecting the Swiss Landeskoordinaten LV03 (CH1903)/Militär-Format (Bern = 600/200 km)³³

³³ All reference coordinates based on the HeliFIS recordings in WGS84 are transformed via web-based swisstopo REFRAME³³ software into Landeskoordinaten LV03. Detailed on the Swisstopo web page <https://www.swisstopo.admin.ch>

Mathematical Proof

Let $f: \mathbb{R} \rightarrow \mathbb{R}$ be a function, which is defined in the following way:

$$f(x) := \begin{cases} ax + b, & \text{if } x \leq t \\ \sqrt{r^2 - (x - x_M)^2}, & \text{if } x \in (t, x_M + r) \end{cases}$$

a, b, r and x_M are real numbers such that f is continuously differentiable at t .

Note. f is composed of a linear function and a function of a semicircle with radius r , whose center has x -coordinate x_M .

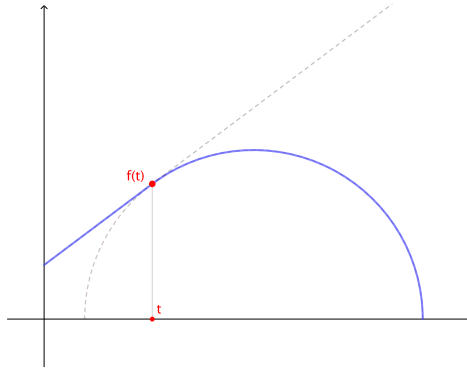


Figure 1: $f(x)$ in blue

Claim. f is not twice differentiable at t .

Proof. Since shifting a function in the coordinate plane does not change the differentiability of the function at a certain point on the curve, we can choose f to be such that the center of the semicircle has coordinates $(0, 0)$. Let $P = (t, p)$ be the point on the semicircle where f changes from a linear function to a function of a semicircle. Then f is defined as:

$$f(x) := \begin{cases} \frac{-t}{\sqrt{r^2 - t^2}}x + p + \frac{t}{\sqrt{r^2 - t^2}}, & \text{if } x \leq t \\ \sqrt{r^2 - x^2}, & \text{if } x \in (t, r) \end{cases}$$

Note. f starts as the function of the tangent to the semicircle at P , where it changes to the function of the semicircle. Thus the function is obviously continuously differentiable at t , with the following derivative:

$$f'(x) = \begin{cases} \frac{-t}{\sqrt{r^2 - t^2}}, & \text{if } x \leq t \\ \frac{-x}{\sqrt{r^2 - x^2}}, & \text{if } x \in (t, r) \end{cases}$$

Excerpt from [8 p 1]:

SCHWEIZERISCHE ZEITSCHRIFT FÜR
VERMESSUNG UND KULTURTECHNIK
Revue technique Suisse des Mensurations et du Génie rural

Herausgeber: Schweiz. Verein für Vermessungswesen und Kulturtechnik. Offiz. Organ der Schweiz. Gesellschaft f. Photogrammetrie

Editeur: Société Suisse de Mensuration et du Génie rural. Organe officiel de la Société Suisse de Photogrammétrie

REDAKTION: Dr. h. c. G. F. BAESCHLIN, Professor, Zollikon (Zürich)

Redaktionschluß: Am 1. jeden Monats

Expedition, Administration und Inseratenannahme:

BUCHDRUCKEREI WINTERTHUR AG., Telefon (052) 2 22 52

Schluß der Inseratenannahme am 6. jeden Monats

NR. 6 • IL. JAHRGANG
der „Schweizerischen Geometer-Zeitung“
Erscheinend am 2. Dienstag jeden Monats
12. JUNI 1951
INSERATE: 25 Rp. per einspalt. mm-Zeile.
Bei Wiederholungen Rabatt gemäß spez. Tarif

ABONNEMENTE:
Schweiz Fr. 15.—, Ausland Fr. 20.— jährlich
Für Mitglieder der Schweiz. Gesellschaft für
Photogrammetrie Fr. 10.— jährlich

Die Klothoide als Übergangskurve im Straßenbau

Von E. Bachmann, dipl. Ing.

Der Übergang von einer Geraden in einen Kreisbogen ist immer sprunghaft, wenn dies auch bei sehr großen Radien oder geringen Fahrgeschwindigkeiten nicht ohne weiteres spürbar ist. Die Eisenbahnen, welche gegen Ende des letzten Jahrhunderts große Fahrgeschwindigkeiten erreichten, begannen schon damals ihre Kurven zu überhöhen und zwischen Gerade und Kreis eine Übergangskurve einzuschalten. Diese, den besonderen Fahreigenschaften der Bahnen angepaßte Übergangskurve ist die sogenannte kubische Parabel.

Measurement arrangements:

- Automatic Flight Inspection System (AFIS) AFIS-220H AFIS – Software Version 6.0.0
- TSO GPS Receiver: GPS4000S (Rockwell Collins) P/N 822-2189-002
- GPS Antenna (TSO GPS) Antcom Active L1/L2 GPS/L-Band
- ANT-532-C 42GO1215A4-XT-1-N FIS GPS Receiver
- Novatel ProPak-OEM4-G2 L1 C/A (Coarse/Acquisition) code (12 channel), L1 and L2 carrier phase and L2 P-code of up to 12 GPS satellites
- GPS Antenna (FIS GPS) Antcom Active L1/L2 GPS/L-Band ANT-532-C 42GO1215A4-XT-1-N
- Positioning: FIS hybrid WADGPS AD-AFIS-220, Differential GPS with Omnistar Solution and INS.

Processed Variables and Heli-FIS Parameter Definitions

run Factor	nr 2 - nr 9
time UTC	
refposGPSWeek	
refposGPSTime	
Y	m see Swiss Topo
X	m see Swiss Topo
refposAlt	ft
refposAltMSL	ft MSL altitude from position reference
refposHorSigPos	m Horizontal Sigma from Positioning System (Truth System) AFIS-220-H
refposVerSigPos	m Vertical Sigma from Positioning System (Truth System) AFIS-220-H
refposTHdg	° True Heading from reference position
refposPitch	° Pitch angle from reference position
refposBank	° Bank angle from reference position
pGPSHErr	m Horizontal RefPos Horizontal GPS 1 SBAS position
pGPSVErr	m Vertical RefPos - Vertical GPS 1 SBAS position
rnavFMSXTD	m RNAV: Cross Track Flight Technical Error from selected FMS (Single GPS Novatel)
rnavAlongNSE	m RNAV:NSE Along Track (Aeronav Single GPS 1Hz)
rnavCrossTSE	m RNAV:TSE Cross Track (Database vs Refpos)
rnavCrossNSE	m RNAV:NSE Cross Track (Aeronav Single GPS 1Hz)
rnavAbsNSE	m RNAV:NSE Absolut (Aeronav Single GPS 1Hz)